SCIENCE CHINA
Chemistry

•ARTICLES•

January 2019 Vol.62 No.1: 95–104
https://doi.org/10.1007/s11426-018-9348-5

Redox-responsive ferrocene-containing poly(ionic liquid)s for antibacterial applications

Tikai Zhang[1], Jiangna Guo[1], Yingying Ding[2], Hailei Mao[2*] & Feng Yan[1*]

[1]*Jiangsu Key Laboratory of Advanced Functional Polymer Design and Application, Department of Polymer Science and Engineering, College of Chemistry, Chemical Engineering and Materials Science, Soochow University, Suzhou 215123, China;*
[2]*Department of Anesthesiology and Critical Care Medicine, Zhongshan Hospital, Fudan University, Shanghai 200032, China*

Received July 12, 2018; accepted August 13, 2018; published online November 5, 2018

Ferrocene (Fc)-containing imidazolium type ionic liquids (ILs) and corresponding poly(ionic liquid) (PIL) membranes with tunable antibacterial activity based on electrochemical redox reaction and host-guest chemistry were developed. The effect of Fc moiety on the antimicrobial activities against both *Staphylococcus aureus* (*S. aureus*) and *Escherichia coli* (*E. coli*) was studied by minimum inhibitory concentration (MIC). The presence of Fc groups highly enhanced the antibacterial efficiency of Fc-containing ILs because of the generation of reactive oxygen species (ROS). The electrochemical oxidation of Fc to Fc^+ and the formation of inclusion complexes between Fc and β-CD via host-guest interactions decreased the antibacterial activities of ILs and PIL membranes. The antibacterial activities may be recovered in some extent upon the electrochemical reduction of Fc^+ to Fc or the exclusion of the Fc out of the cavity of β-CD. Furthermore, all the Fc-containing PIL membranes showed relatively low hemolysis activities and none cytotoxicity toward human cells, indicating clinical feasibility in topical applications.

antibacterial activities, imidazolium cations, ferrocene, poly(ionic liquid), cytotoxicity

Citation: Zhang T, Guo J, Ding Y, Mao H, Yan F. Redox-responsive ferrocene-containing poly(ionic liquid)s for antibacterial applications. *Sci China Chem*, 2019, 62: 95–104, https://doi.org/10.1007/s11426-018-9348-5

1 Introduction

Bacterial infections are one of the leading causes of morbidity in hospitalized patients, especially antibiotic-resistant bacterial infections caused by the overuse of antibiotics [1,2]. Therefore, development of antibacterial agents without inducing resistance is urgent and has attracted special interest in the area of healthcare [3]. Natural antibacterial agents, inorganic and organic antibacterial materials [4], including silver-based materials [5,6], cationic compounds [7,8], chitosan [9] and nano-antibacterial materials [10,11], have been recently developed or synthesized. The antibacterial mechanisms of these agents are variant, ranging from disrupting the cell integrity to inhibit the cell metabolism. Among the antimicrobial materials investigated, cationic compounds (or polymers) containing quaternary ammonium [12], phosphonium [13], pyridinium [14] or imidazolium cations [15], have been extensively studied due to their broad-spectrum antibacterial properties as well as low toxicity. These cationic compounds (or polymers) can damage the bacteria cells through the electrostatic and hydrophobic interactions, which endows these agents a type of ideal materials for antimicrobial applications without developing resistance by bacteria. On the other hand, accumulation of active antibacterial agents highly increased the bacterial resistance from a view of long-term applications [16,17].

*Corresponding authors (email: mao.hailei@zs-hospital.sh.cn; fyan@suda.edu.cn)

Therefore, Zhang and coworkers [18] fabricated polypseudorotaxanes with controlled antibacterial activity based on cationic polymers. The antibacterial efficiency could be controlled by the content of cucurbit[7]uril [19–21]. Wei and coworkers [22] fabricated multifunctional and regenerable antibacterial surfaces containing guest moieties, which can be further used to incorporate biocidal host molecules. However, controlling the antimicrobial activity of antimicrobial agents is still a significant challenge.

Ionic liquids (ILs) are organic salts comprised of cations and anions, with special inherent conductivity and high chemical stability [23]. Ionic liquids (ILs) and poly(ionic liquid)s (PILs) have been used in the field of bioengineering and biomaterials [24]. More recently, the imidazolium [25], pyrrolidinium [7] and quaternary ammonium cations [26,27] based ILs have been used as antibacterial materials because of the electrostatic interaction between the anionic bacterial cell wall and the cations of the ILs.

Ferrocene (Fc), an organometallic compound with aromatic nature, has gained a great deal of both industrial and academic attentions [28]. Fc-containing compounds have been widely used in biological applications because of their unique biological properties, such as low toxicity, small size and relative lipophilic property, as well as high thermal and soluble stability [29,30]. For example, Fc-containing compounds have been applied for the synthesis of antimicrobial inhibition multilayer coatings via host-guest interaction chemistry [31]. Chen and co-workers [32] synthesized Fc-containing penicillin which showed comparable activity to benzyl penicillin. However, applications of Fc-containing compounds are restricted due to their poor water solubility [33]. Recently, several strategies and formulations have been used to increase the solubility and bioavailability of the Fc-containing materials in water, such as complexing with cyclodextrins (CD) [34], adding co-solvents [35], conjugation with dendrimers [36] or forming ferrocenyl derivatives with ILs. However, the application of Fc as antimicrobial materials has been rarely studied.

Herein, a series of Fc-containing imidazolium-type ILs and PIL membranes with tunable antibacterial activities were synthesized. The antibacterial activities of the IL small molecules against both *Staphylococcus aureus* (*S. aureus*) and *Escherichia coli* (*E. coli*) were investigated by determination of the minimum inhibitory concentration (MIC). The tunable antimicrobial activities of the ILs were modulated by the redox state of the Fc moieties via applied voltage, as well as the molecular recognition between β-cyclodextrin (β-CD) and Fc moieties. Meanwhile, the modulated antibacterial properties of PIL membranes prepared by crosslinking of imidazolium-type IL monomers with acrylonitrile and styrene were further studied. In addition, the hemolysis and cytotoxicity of the PIL membranes were investigated systematically.

2 Experimental

2.1 Materials

1-Vinylimidazolium, 3-bromo-1-propanol, 6-bromo-1-hexanol and 9-bromo-1-nonanol, ferrocenecarboxylic acid (Fc-COOH), 4-dimethylaminopyridine (DMAP), *N*,*N*-dicyclohexylcarbodiimide (DCC), Luria-Bertani broth medium (LB), poly(ethylene terephthalate) (PET), deuterium oxide (D_2O) and chloroform-d ($CDCl_3$) were analytic grade and used as received without further purification. 2,2-Azobisisobutyronitrile (AIBN, 98%) was recrystallized from ethanol and kept in refrigerator before use. *S. aureus* (ATCC 6538) and *E. coli* (8099) strains were kindly provided by Dr. Shengwen Shao (Huzhou University School of Medicine, China). Deionized water was used throughout all the experiments. Singlet Oxygen Sensor Green was obtained from Invitrogen (Thermo Fisher Scientific, USA).

2.2 Characterization

^{1}H NMR and ^{13}C NMR spectra were recorded on a Varian 400 MHz spectrometer using D_2O or $CDCl_3$ as the solvents. The turbidity of the bacteria suspension was recorded by a microplate reader. The hemoglobin release was recorded by the OD values at 576 nm tested by the Eon microplate spectrophotometers (BioTek Instruments, Inc., USA). A field-emission scanning electron microscope (SEM, Hitachi Model S-4700, Japan) was used to observe the morphology of the bacteria on the surfaces of PET and the synthesized PIL membranes. Fourier transform infrared (FT-IR) spectra of the membrane was recorded by a Thermo scientific Nicolet 6700 FT-IR spectrometer (4000–400 cm^{-1}) (USA). X-ray photoelectron spectroscopy (XPS) tests were performed using an XPS-7000 spectrometer (Rigaku, Japan) equipped with a Mg KaX-ray source. Fluorescence spectra were obtained using a HITACHI F-2500 spectrometer (Japan).

2.3 Synthesis of *n*-(1-hydroxyalkyl)-1-vinylimidazolium bromide (IL-C_n-OH)

n-(1-Hydroxyalkyl)-1-vinylimidazolium bromide (IL-C_n-OH) was synthesized via the reaction of equimolar amount of 3-bromo-1-alkyl alcohol and 1-vinylimidazolium at the room temperature for 6 h. The product was washed with diethyl ether three times and then dried under vacuum at room temperature to obtain a white powder.

3-(1-Hydroxypropyl)-1-vinylimidazolium bromide (IL-C_3-OH) (yield 85%), ^{1}H NMR (400 Hz, D_2O, δ): 9.09 (s, 1H), 7.79 (s, 1H), 7.61 (s, 1H), 7.15 (m, 1H), 5.81 (m, 1H), 5.43 (d, 1H), 4.36 (t, 2H), 3.65 (t, 2H), 2.15 (m, 2H). ^{13}C NMR (400 MHz, D_2O, δ): 131.91, 125.56, 120.27, 116.87, 106.73, 55.21, 44.24, 28.80. HRMS [ESI] calcd for $C_8H_{13}ON_2$ $[M]^+$ 153.2011, found 153.1010.

3-(1-Hydroxyhexyl)-1-vinylimidazolium bromide (IL-C_6-OH) (yield 82%), ^{1}H NMR (400 MHz, D_2O, δ): 9.54 (s, 1H), 8.19 (s, 1H), 7.96 (s, 1H), 7.26 (m, 1H), 5.91 (d, 1H), 5.38 (d, 1H), 4.68 (s, 2H), 4.45 (s, 2H), 4.32 (t, 2H), 4.19 (s, 8H), 2.21 (m, 2H). ^{13}C NMR (400 MHz, D_2O, δ): 128.16, 122.78, 119.33, 109.23, 102.66, 61.50, 49.79, 30.99, 28.96, 24.93, 24.39. HRMS [ESI] calcd for $C_{11}H_{19}ON_2$ $[M]^+$ 195.2806, found 195.1496.

3-(1-Hydroxynonyl)-1-vinylimidazolium bromide (IL-C_9-OH) (yield 92%), ^{1}H NMR (400 MHz, D_2O, δ): 9.06 (s, 1H), 7.79 (s, 1H), 7.59 (s, 1H), 7.15 (m, 1H), 5.88–5.74 (d, 1H), 5.43 (d, 1H), 4.25 (t, 2H), 3.59 (t, 2H), 1.91 (d, 2H), 1.53 (d, 2H), 1.31 (d, 11H). ^{13}C NMR (400 MHz, D_2O, δ): 128.08, 122.81, 119.35, 109.26, 102.75, 61.75, 49.89, 31.31, 29.03, 28.43, 28.38, 27.98, 25.27, 24.99. HRMS [ESI] calcd for $C_{14}H_{25}ON_2$ $[M]^+$ 237.3601, found 237.1972.

2.4 Synthesis of *n*-bromo-1-ferrocenecarboxylate (FcC_nBr)

The FcC_nBr was synthesized by esterification reaction according to the earlier report [37]. Fc-COOH (5.40 mmol) was dissolved in 80 mL $CHCl_3$, followed by adding bromoalkyl alcohol (3.60 mmol) dropwise and stirred at the room temperature. After 2 h, DCC (3.60 mmol) and DMAP (1.80 mmol) were added into the above solution and stirred for another 36 h. Removed the insoluble salts by filtration and purified the product by silica gel column chromatography using ethyl acetate/petroleum ether (1:100, *v*/*v*) as eluent. Afterwards, the solvent was dried by rotary evaporate to obtain the target product.

3-Bromo-1-ferrocenecarboxylate (FcC_3Br) (yield 62%), ^{1}H NMR (400 MHz, $CDCl_3$, δ): 10.30 (s, 2H), 7.85 (s, 2H), 7.46 (s, 2H), 7.39 (t, 2H), 6.60 (t, 2H), 5.31 (p, 2H), 4.46–4.19 (m, 2H) .

6-Bromo-1-ferrocenecarboxylate (FcC_6Br) (yield 70%), ^{1}H NMR (400 MHz, $CDCl_3$, δ): 10.32 (s, 2H), 7.87 (s, 2H), 7.45 (s, 2H), 6.49 (t, 2H), 5.18–4.88 (m, 2H), 5.34 (d, 2H), 4.56 (s, 4H), 4.33 (d, 1H).

9-Bromo-1-ferrocenecarboxylate (FcC_9Br) (yield 58%), ^{1}H NMR (400 MHz, $CDCl_3$, δ): 10.31 (s, 2H), 7.86 (s, 2H), 7.44 (s, 2H), 7.39–7.30 (m, 2H), 4.46 (d, 1H), 4.40 (t, 4H), 4.31 (d, 3H), 3.93 (m, 1H).

2.5 Synthesis of 3-{*n*-[(ferrocene-methanoyl)oxy]alkyl}-1-vinylimidazolium bromide (IL-C_n-Fc)

Equimolar amount of FcC_nBr was mixed with 1-vinylimidazolium and stirred for 6 h at room temperature. Afterwards, diethyl ether was used to wash the raw product three times to remove the impurity and dried under vacuum at room temperature to obtain target product.

3-{3-[(Ferrocene-methanoyl)oxy]propyl}-1-vinylimidazolium bromide (IL-C_3-Fc) (yield 80%), ^{1}H NMR (400 MHz, $CDCl_3$, δ): 9.54 (s, 1H), 8.19 (s, 1H), 7.96 (s, 1H), 7.26 (m, 1H), 5.91 (d, 1H), 5.38 (d, 1H), 4.68 (s, 2H), 4.45 (s, 2H), 4.32 (t, 2H), 4.19 (s, 7H), 2.31–2.05 (m, 2H). ^{13}C NMR (400 MHz, D_2O, δ): 174.79, 128.09, 122.84, 119.57, 109.52, 102.51, 72.61, 69.96, 62.26, 47.56, 28.12. HRMS [ESI] calcd for $C_{19}H_{21}O_2N_2Fe$ $[M]^+$ 371.1554, found 371.1971.

3-{6-[(Ferrocene-methanoyl)oxy]hexyl}-1-vinylimidazolium bromide (IL-C_6-Fc) (yield 72%), ^{1}H NMR (400 MHz, $CDCl_3$, δ): 8.79–8.45 (m, 1H), 7.27 (d, 1H), 7.03 (s, 1H), 6.35 (m, 1H), 5.01 (d, 1H), 4.46 (t, 2H), 3.93–3.69 (m, 3H), 3.60 (d, 3H), 3.23 (d, 3H), 1.75–1.36 (m, 7H), 0.98 (m, 3H), 0.82–0.70 (m, 3H), 0.59–0.34 (m, 7H), 0.17 (t, 3H). ^{13}C NMR (400 MHz, D_2O, δ): 173.28, 128.02, 122.75, 119.42, 109.34, 102.46, 71.93, 70.40, 70.12, 69.84, 64.80, 49.70, 29.24, 28.13, 25.27, 24.96. HRMS [ESI] calcd for $C_{22}H_{27}O_2N_2Fe$ $[M]^+$ 407.1449, found 407.1442.

3-{9-[(Ferrocene-methanoyl)oxy]nonyl}-1-vinylimidazolium bromide (IL-C_9-Fc) (yield 85%), ^{1}H NMR (400 MHz, $CDCl_3$, δ): 9.33 (d, 1H), 8.27–7.98 (m, 1H), 7.98–7.64 (m, 1H), 7.15 (d, 1H), 5.82 (m, 2H), 5.30 (d, 2H), 4.62 (d, 3H), 4.41 (s, 3H), 4.23–3.90 (m, 15H), 1.73 (s, 4H), 1.53 (d, 3H), 1.40–0.92 (m, 21H). ^{13}C NMR (400 MHz, D_2O, δ): 174.70, 136.63, 129.21, 128.32, 127.89, 122.84, 119.56, 116.66, 109.53, 102.47, 72.59, 69.96, 68.73, 65.91, 62.21, 47.53, 28.14, 14.04. HRMS [ESI] calcd for $C_{25}H_{33}O_2N_2Fe$ $[M]^+$ 449.2244, found 449.1874.

2.6 Preparation of imidazolium-based poly(ionic liquid) (PIL) membranes

In order to investigate the influence of the Fc redox form on the antibacterial activities, IL-C_6-Fc was chosen as a representative to prepare the PIL membranes because of its suitable antibacterial activity. Briefly, in order to obtain PIL membranes with good antibacterial activity and excellent mechanical property, a mixture containing IL-C_6-Fc (20 wt%), styrene (15 wt%), acrylonitrile (65 wt%), and AIBN (1 wt% to the formulation based on the total weight) (divinyl benzene as a crosslinker) were used to prepare the membranes. The mixture was ultrasonicated to homogeneous solution, which was initiated and polymerized to form a membrane at 75 °C for 6 h in a glass mold. Subsequently, the obtained PIL membranes (~100 μm in thickness) were ultrasonicated in deionized water and washed with ethanol at room temperature for 24 h to remove the unreacted monomers. The membrane was dried in oven before characterization.

2.7 Bacteria culture

E. coli and *S. aureus* were cultured in LB broth medium at 37 °C up to the exponential growth phase. OD_{600} was mea-

sured to determining the bacterial concentration. The bacterial suspending solutions (OD_{600}=0.1) were used to characterize the antibacterial properties of imidazolium-based ILs.

2.8 Minimum inhibitory concentration (MIC) test

MIC values were measured to investigate the antibacterial activities of imidazolium-type ILs in the way of broth microdilution format in accordance with Clinical & Laboratory Standards Institute guidelines. The 96-well plates were incubated at 37 °C and tested the optical density (OD) at set intervals with a microplate reader. MIC50 is the minimum ILs concentration that can inhibit 50% of bacterial growth after incubating for 24 h at 37 °C.

2.9 Antibacterial activities of synthesized PIL membranes

The bacterial suspension was incubated on the sterilized PET (as negative control) and PIL membrane (1.5 cm×1.5 cm) for 4 h at 37 °C. Afterwards, 10 μL bacterial suspension was transferred and smeared onto a LB agar plate evenly to record the number of visible bacterial colonies after incubated for 24 h at 37 °C. Each colony assay test was repeated at least three times. The antibacterial rate was calculated with the following formula (*A* and *B* represent the number of viable colonies of the control and experimental sample, respectively):

$$\text{Antibacterial rate (\%)}=\frac{A_{\text{negative control}}-B_{\text{sample}}}{A_{\text{negative control}}}\times 100\%$$

2.10 Redox regulation of ILs and PIL membranes

The antibacterial activities of the ILs and PIL membranes were modulated by the applied potential and the addition of β-CD. In brief, IL-C_6-Fc was oxidized to IL-C_6-Fc^+ at +2 V voltage in deionized water. Besides, the adscititious β-CD could include the Fc units in the IL-C_6-Fc through the host-guest interactions to form IL-C_6-Fc-CD. After the oxidation of IL-C_6-Fc-CD with an applied +2 V potential, the Fc units could be excluded from the cavity of the β-CD to form IL-C_6-Fc^+-CD. The regulating process of PIL membranes was conducted as the similar method described above.

2.11 Morphological changes of the bacteria

The morphological changes of the bacteria incubated on the PIL membrane surfaces were observed by SEM. The bacterial suspension (OD_{600}=0.1) of *E. coli* or *S. aureus* was dropped onto the surface of sterilized PIL membranes and incubated for 4 h at 37 °C with PET as control. Afterwards, the membranes were immersed in 2.4 wt% glutaraldehyde solution for 2 h, followed by dehydrating gradiently with 10 vol%, 20 vol%, 30 vol%, 40 vol%, 50 vol%, 60 vol%, 70 vol%, 80 vol%, 90 vol% and 100 vol% ethanol solutions for 15 min of each step.

2.12 Singlet oxygen ($^1O_2$) test

The singlet oxygen produced by ILs and PIL membranes was tested. Briefly, ILs (30 mg) were dissolved in the ultrapure water (3 mL) completely, followed by adding 10 μL of Singlet Oxygen Sensor Green. The emission spectrums were recorded with the fluorescence spectrometer (λ_{ex}=494 nm) after ultrasonicating for 10 min. In order to investigate the singlet oxygen generated by PIL membranes, a piece of PIL membrane (1.0 cm×1.0 cm) was immersed into ultrapure water (3 mL) for 30 min firstly, and then 10 μL of Singlet Oxygen Sensor Green was added into the ultrapure water and incubated with the PIL membranes for 10 min. The emission spectrums of the samples were recorded at λ_{ex}=494 nm.

2.13 Hemolysis assay

The red blood cells were prepared by the centrifugation of fresh human blood at 1500 r/min for 15 min and washed with phosphate buffered saline (PBS) until the supernatant liquid was pellucid. Then 2 vol% red blood cells diluted with PBS was incubated with the sterilized PET and PIL membranes (1.0 cm×1.0 cm) (5 mL for each tube) at 37 °C for 3 h, respectively. About 100 μL supernatant obtained by centrifuged the diluted blood samples at 1500 r/min for 15 min was transferred into a 96-well plate. The OD_{576} was recorded with the Eon microplate spectrophotometers (Bio Tek Instruments, Inc.) to evaluate the hemoglobin release. The red blood cells in PBS and with 2 % Triton were used as the negative and positive control, respectively. The hemolysis rate was calculated on the basis of the following formula:

$$\text{Hemolysis rate (\%)}=\frac{\text{OD}_{\text{sample}}-\text{OD}_{\text{negative control}}}{\text{OD}_{\text{positive control}}-\text{OD}_{\text{negative control}}}\times 100\%$$

2.14 Cytotoxicity evaluation

The regulation for separating and culturing the human dermal fibroblasts (offered by Shanghai Ninth People's Hospital, China) was followed with the processes reported in [38]. 3-(4,5-Dimethylthiazol-2-yl)-2,5-diphenyltetrazolium bromide (MTT) assay was used to evaluate the toxicity of PIL membranes against human dermal fibroblasts. Briefly, human dermal fibroblasts (1×10^4) were cultured in 10% fetal calf serum medium in a 24-well plate for 48 h, and followed by adding PET and PIL membranes (1.0 cm×1.0 cm) into the

fibroblast cell solutions and cultured at 37 °C. After 72 h, 0.1 mL of MTT solution (5 g/L in PBS) was added into each well and incubated at 37 °C for another 4 h. Then, 0.75 mL dimethyl sulfoxide (DMSO) was added into each well to dissolve the formazan crystals after the removal of the supernatant liquid. The OD_{490} was recorded to evaluate formazan release with the Eon microplate spectrophotometer (Bio Tek Instruments, Inc., USA). All the tests were repeated for three times at least. The relative growth rate (RGR) of the human dermal fibroblast cells was calculated on the basis of the following formula:

$$\text{RGR}\ (\%)=\frac{OD_{sample}}{OD_{control}}\times 100\%$$

3 Results and discussion

In order to investigate the effect of Fc moiety on the antibacterial activities of imidazolium-based IL small molecules, analogous structures were synthesized: 3-(1-hydroxypropyl)-1-vinylimidazolium bromide (IL-C_3-OH), 3-(1-hydroxyhe-xyl)-1-vinylimidazolium bromide (IL-C_6-OH), 3-(1-hydroxynonyl)-1-vinylimidazolium bromide (IL-C_9-OH), 3-{3-[(ferrocene-methanoyl)oxy] propyl}-1-vinylimidazolium bromide (IL-C_3-Fc), 3-{6-[(ferrocene-methanoyl) oxy]hexyl}-1-vinylimidazolium bromide (IL-C_6-Fc), 3-{9-[(ferrocene-methanoyl)oxy]nonyl}-1-vinylimidazolium bromide (IL-C_9-Fc) (see Scheme 1, and Scheme S1 in the Supporting Information online). The chemical structure and purity of all the synthesized IL small molecules were confirmed by ^{1}H NMR, ^{13}C NMR spectra and high-resolution MS data, indicating the successful synthesis of all the target compounds. All the synthesized ILs were further characterized by FT-IR spectra, as shown in Figure S1 (Supporting Information online). The absorption peaks at 1169 cm^{-1} of IL-C_n-OH (n=3, 6, 9) were assigned to –C–O–, while the stretching vibration peaks of imidazolium cations appeared at 1649 cm^{-1} (Figure S1(A)). As for the IL-C_n-Fc (n=3, 6, 9), the characteristic peak of ferrocene groups arises at 1250 cm^{-1} (Figure S1(B)), which confirms the successful synthesis of IL-C_n-Fc.

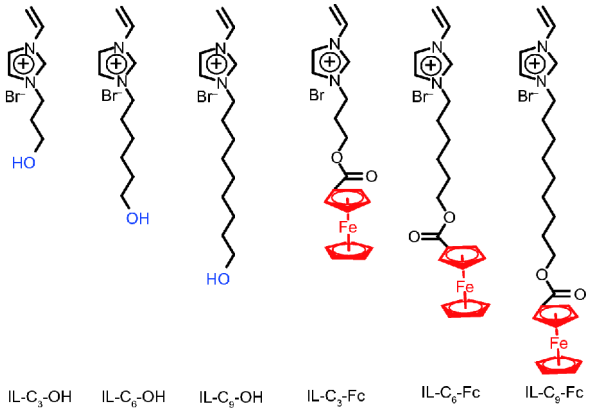

Scheme 1 The chemical structures of the synthesized imidazolium-type IL small molecules (color online).

The antibacterial activities of the imidazolium-based IL small molecules were tested with Gram-negative *E. coli* and Gram-positive *S. aureus* as model microorganisms by minimum inhibitory concentration (MIC50), which indicates the lowest concentration that can inhibit 50% growth of microorganisms after 24 h incubation. The MIC50 values were summarized and listed in Table 1. It can be clearly seen that all of the ILs synthesized in this work showed antibacterial activities against both *E. coli* and *S. aureus*. It is speculated that the antibacterial activities may be induced by the electrostatic interactions between the imidazolium cationic groups and the electronegative phosphate of the cell walls, which may destroy the integrity of the cell membranes. Meanwhile, the insertion of the hydrophobic aliphatic chains into the hydrophobic regions of the lipid membrane of bacteria may cause the leakage of the electrolyte in the cell and result in the cell death [7,8]. In addition, the MIC50 values were affected by the alkyl chain length substituted at the N3 position of imidazolium cations. The longer alkyl chain length, the lower the MIC50 value is, indicating the higher antibacterial efficiency of ILs. It is considered that the hydrophobic interaction between the alkyl chain and the cell walls increased with the incremental alkyl chain length, leading to the higher antibacterial activities [39,40]. It should be noted that the antibacterial activities of ILs are also correlated to the Fc moiety substituted to the imidazolium cations. The MIC50 values of the ILs containing Fc groups were highly decreased if compared with the ILs with the same alkyl chain length for both *E. coli* and *S. aureus*, indicating the enhancement of the antibacterial activities (Table 1). It is supposed that the introduced Fc group can produce reactive oxygen species (ROS), such as singlet oxygen ($^1O_2$), which may lead to the progressive oxidative damage of the bacterial cell wall (or membrane). Figure 1(c, d) shows the fluorescence spectra of SOSG with the existence of IL-C_n-OH and IL-C_n-Fc (n=3, 6, 9) in ultrapure water. SOSG is used as the probe of the

Table 1 Antibacterial activities of imidazolium-based IL small molecules measured as MIC50

Samples	MIC50 (μmol/mL)	
	S. aureus	*E. coli*
IL-C_3-OH	34.40	40.04
IL-C_6-OH	9.02	17.13
IL-C_9-OH	3.06	3.74
IL-C_3-Fc	7.28	13.77
IL-C_6-Fc	2.60	3.05
IL-C_9-Fc	0.08	0.39

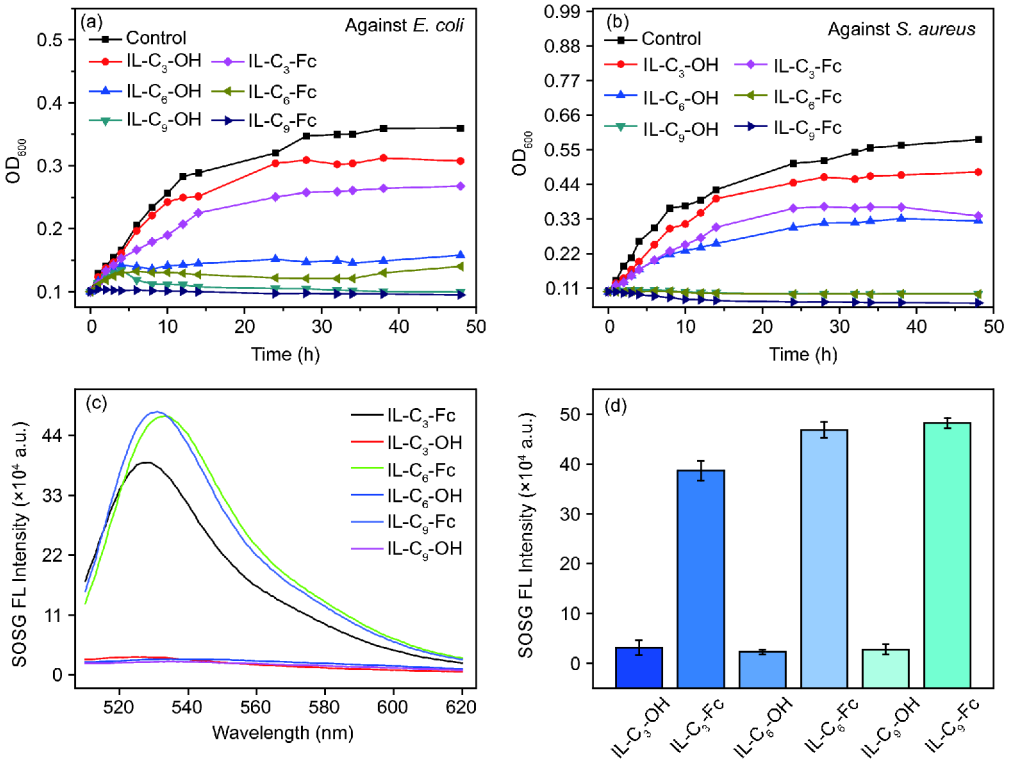

Figure 1 Growth curves of bacteria incubated with imidazolium-based IL small molecules under the concentration of individual MIC50 for 48 h against (a) *E. coli* and (b) *S. aureus*. (c) The emission spectrums (λ_{ex}=494 nm) and (d) fluorescence intensity of SOSG (λ_{em}=530 nm) with the existence of ILs in ultrapure water (color online).

generated $^1O_2$. As it can be seen that all of the ILs can generate $^1O_2$ in water under visible light. However, introduction of Fc groups obviously improved the $^1O_2$ generation. Therefore, it is not surprising that the ILs with Fc groups showed the better antibacterial activity because of the synergistic attributes of the ILs and Fc groups. It should be noted that the antibacterial activities of all the ILs against *E. coli* were worse than that of *S. aureus*. Such a difference may be induced by the different bacterial cell walls [41,42]. The cell wall of the *E. coli* includes an outer membrane (7–8 nm) and a peptidoglycan inner layer (2–7 nm), while the cell membranes of *S. aureus* is a thick (20–80 nm) and porous peptidoglycan layer, which interconnects with the negatively charged teichoic acid [43,44]. Compared with the imperforate *E. coli*, the hydrophobic alkyl chains are easier to insert into the porous cell wall of *S. aureus* and destroy the peptidoglycan layer to cause the bacteria die [45,46].

The growth curves of bacteria incubated with IL small molecules under MIC50 values were further investigated by microplate reader, as shown in Figure 1(a, b). After contacting with ILs for 48 h, the OD_{600} values of *S. aureus* and *E. coli* incubated with imidazolium-based ILs small molecules were lower than that of the control, especially for the Fc-containing ILs. The results indicated that the imidazolium-based ILs could inhibit (or kill) the bacteria growth.

The morphology changes of *S. aureus* and *E. coli* incubated with the synthetic ILs were characterized by scanning electron microscopy (SEM) (Figure 2). It can be seen that the bacteria cell surfaces on the PET membranes were complete and smooth (Figure 2(A-a, B-a)). However, aggregations of lipid vesicles, distorted and collapsed bacterial membranes were observed on the surfaces of PET membranes cultured with ILs (Figure 2(A-b–A-g, B-b–B-g)). The results further confirmed the antibacterial activities of the ILs against both *S. aureus* and *E. coli*.

How can we realize control over antibacterial activity using Fc-containing ILs? By electrochemical oxidation and host-guest complexation, the Fc groups can be oxidized to Fc^+ or complexed with β-CD, and thus may lead to the lower antibacterial efficiency. To confirm this assumption, firstly, electrochemical oxidation reaction of ILs was used to control the antibacterial properties. The MIC values were tested to determine the antibacterial properties (Table 2). Upon the electrochemical oxidation of Fc to Fc^+ at +2 V (confirmed by X-ray photoelectron spectroscopy (XPS), Figure S2), the MIC50 values against *E. coli* and *S. aureus* were increased from 0.99 to 3.70 μmol/mL, and from 0.43 to 0.93 μmol/mL for IL-C_6-Fc and IL-C_6-Fc^+, respectively. The results indicated that the oxidation of the Fc group decreased the antibacterial activities of corresponding ILs. Such a difference may be due to the different reactive oxygen species (ROS) content generated by Fc (or Fc^+) moieties, since the

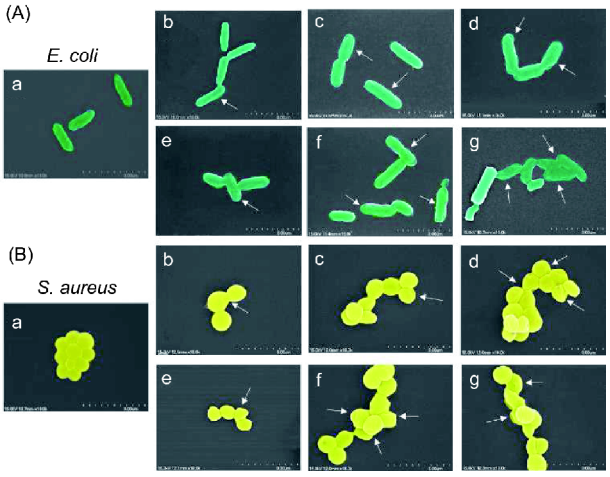

Figure 2 Scanning electron microscopy (SEM) images of *E. coli* (A) and *S. aureus* (B) incubated with IL small molecules for 4 h. (a) PET; (b) IL-C_3-OH; (c) IL-C_6-OH; (d) IL-C_9-OH; (e) IL-C_3-Fc; (f) IL-C_6-Fc; (g) IL-C_9-Fc. Collapses and fusion of bacterial cell membranes incubated with IL small molecules are observed (indicated by white arrows). The concentration of the ILs incubated with bacterial cells was MIC50 (color online).

ROS would lead to the oxidative damage of the bacterial cell membrane (or wall) [47]. Figure 3(a) shows the fluorescence spectra of SOSG, the probe of $^1O_2$, with the existence of IL-C_6-Fc, IL-C_6-Fc$^+$, IL-C_6-Fc-CD and IL-C_6-Fc$^+$-CD in ultrapure water. Both IL-C_6-Fc and IL-C_6-Fc$^+$ can generate $^1O_2$ in water under visible light. The $^1O_2$ concentration generated by IL-C_6-Fc was higher than that of IL-C_6-Fc$^+$. Therefore, it is not surprising that the IL-C_6-Fc showed relatively higher antibacterial activity than IL-C_6-Fc$^+$. Furthermore, the host-guest interaction was used to modulate the antibacterial activities. It has already been demonstrated that β-CD is able to form inclusion complex with Fc groups through host-guest interaction [48]. Upon the addition of β-CD, the MIC values increased from 0.99 μmol/mL for IL-C_6-Fc to 7.34 μmol/mL for IL-C_6-Fc-CD against *E. coli*, and from 0.43 to 1.58 μmol/mL against *S. aureus*, respectively (Table 2). It is speculated that the Fc moieties can be encapsulated into the hydrophobic cavity of the β-CD, which would reduce the mobility of hydrophobic segments and weaken the hydrophobic interaction between the ILs and the bacterial phos-

Table 2 The modulated bactericidal activity of the Fc-containing ILs measured as MIC50

Samples	MIC50 (μmol/mL)	
	S. aureus	*E. coli*
IL-C_6-Fc	0.43	0.99
IL-C_6-Fc$^+$	0.93	3.70
IL-C_6-Fc-CD	1.58	7.34
IL-C_6-Fc$^+$-CD	1.17	3.84

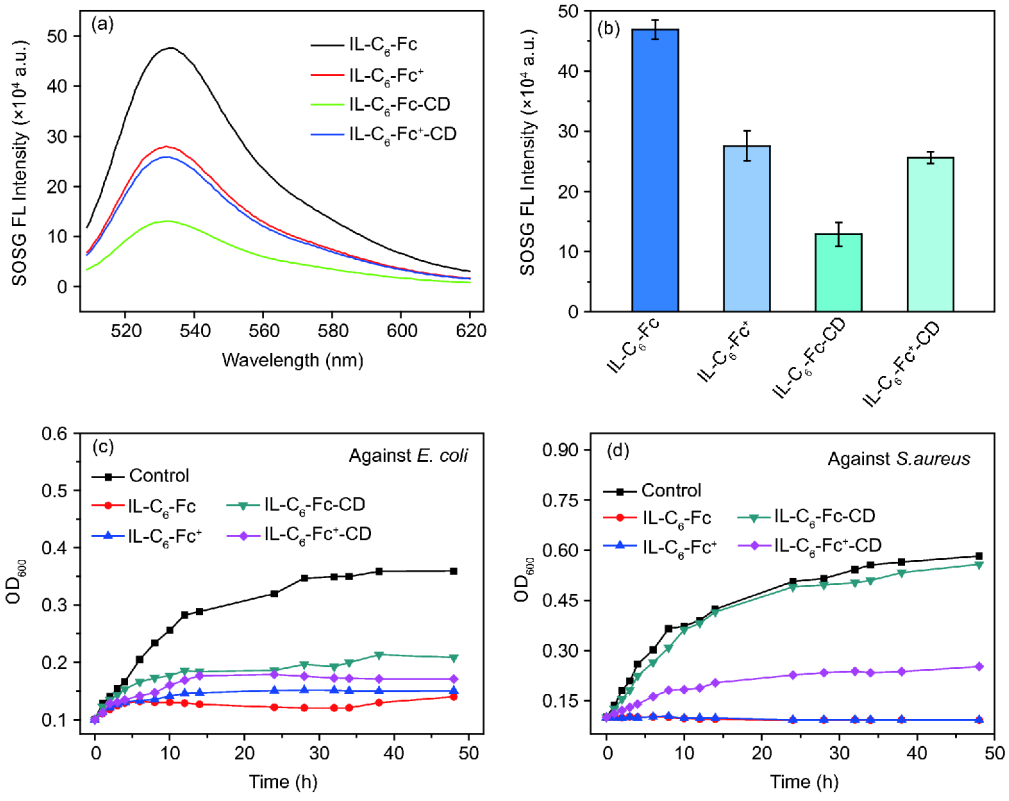

Figure 3 (a) The emission spectrums (λ_{ex}=494 nm) and (b) fluorescence intensity of SOSG (λ_{em}=530 nm) with the existence of ILs in ultrapure water. Growth curves of bacteria incubated with Fc-containing IL small molecules modulated by the redox state of Fc and the addition of β-CD under the concentration of individual MIC50 for 48 h against (c) *E. coli* and (d) *S. aureus* (color online).

pholipid bilayers. Besides, the formation of the inclusion compound (Fc/β-CD) may lead to the decrease of the ROS generated by Fc (Figure 3(b)). Therefore, the antibacterial activities of ILs were decreased. Upon applying +2 V, the IL-C_6-Fc-CD was oxidized to IL-C_6-Fc^+-CD, the MIC50 against *S. aureus* decreased from 1.58 μmol/mL for IL-C_6-Fc-CD to 1.17 μmol/mL for IL-C_6-Fc^+-CD (Table 2), indicating that the antibacterial activity was increased. The Fc^+ moiety has a lower binding affinity with β-CD than that of Fc, which makes the Fc/β-CD inclusion complex diminish. The naked Fc^+ may interacted with bacterial through electrostatic interaction and increase the antibacterial efficiency. Simultaneously, the ROS produced by the IL-C_6-Fc^+-CD system is higher than that of the IL-C_6-Fc-CD (Figure 3(a, b)), which may also contribute to the improvement of the antibacterial properties. The MIC50 values of IL-C_6-Fc^+-CD were slightly higher than those of IL-C_6-Fc^+ probably due to the partial oxidation of Fc. The results also indicated that the Fc-containing ILs not only exhibited modulated antibacterial activities upon electrochemical redox reaction and the host-guest interactions with β-CD, but also showed reversible antibacterial behavior upon those stimuli.

The growth curves of bacteria incubated with Fc-containing ILs, under different modulated conditions were also tested by microplate reader (Figure 3(c, d)). The OD_{600} values of the bacteria cultured with Fc-containing ILs kept lower than that of the control bacteria during 48 h tests, which is IL-C_6-Fc>IL-C_6-Fc^+>IL-C_6-Fc^+-CD>IL-C_6-Fc-CD. The result further confirmed the antibacterial activities of IL-C_6-Fc could be modulated.

Intrinsically antimicrobial polymeric membranes with robust mechanical properties have a wide range of prospects in practical applications. Here, antibacterial PIL membranes were prepared by co-polymerized with styrene and acrylonitrile to strengthen the chemical resistance [49], and mechanical property of the PIL membrane, as described in Scheme 2. The chemical structures of PIL-C6-Fc membrane were characterized by FT-IR spectra (Figure S3(A)). The PIL membrane shows an absorption band of cyano groups (C≡N) at about 2340 cm^{-1}, and the bending vibration peak of $–CH_3–$ and $–CH_2–$ appears at 2945 cm^{-1}. The absorption peaks at 1300–1000 and 1715 cm^{-1} are assigned to –CO and –C=O of ester group, respectively. The characteristic peak of benzene rings arises at 1600 cm^{-1}. The absorption peak at 3300–3400 cm^{-1} of PIL-C_6-Fc-CD membrane is assigned to the –OH of β-CD, and the absorption peak at 1180 cm^{-1} is arose by –CO– of β-CD in the PIL-C_6-Fc-CD membrane. The FT-IR spectra indicate that the imidazolium-based PIL membrane is synthesized successfully. In addition, all the PIL-C_6-Fc membrane surfaces are uniform and smooth, without any visible pore from SEM (Figure S3(B)).

The redox-responsive antibacterial properties of the PIL-C_6-Fc membrane were also investigated and the modulated

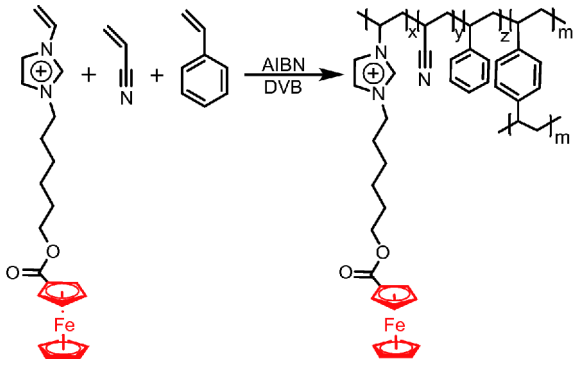

Scheme 2 Schematic representation of the synthesis of PIL-C_6-Fc membrane (color online).

process is similar to that of the IL small molecules. The antibacterial activity results are consistent with those of the ILs small molecules, as shown in Figure 4(a, b), that is, PIL-C_6-Fc-CD<PIL-C_6-Fc^+-CD<PIL-C_6-Fc^+<PIL-C_6-Fc. With the oxidation of Fc to Fc^+, the bacterial viability was highly increased for *E. coli* (from about 20% to 53%), while the bacterial viability was increased from ~20% to nearly 100% for *E. coli* with the addition of β-CD. Similar tunable antibacterial properties were observed for *S. aureus*. The results should be attributed to the generation of ROS. Figure 4(c) showed the fluorescence spectrums of all the PIL membrane samples obtained at λ_{ex}=494 nm. The ROS generated by PIL-C_6-Fc was higher than that of the PIL-C_6-Fc^+, once the Fc moieties were included into β-CD, the fluorescence intensity decreased obviously (Figure 4(d)). The SEM images further confirmed the antibacterial properties of the PIL membranes (Figure S4).

Good biocompatibility of antibacterial materials is essential for their practical applications. Here, the hemocompatibility of the synthesized imidazolium-based PIL membranes under different conditions was characterized by the hemolysis rate toward fresh human red blood cells (RBCs), and the results are listed in Table 3. It can be seen that all the PIL membranes with different antibacterial activities showed extremely low hemolytic activities (<0.5%) for RBCs. According to the standard for the non-direct contact biomedical materials (hemolysis rate<5%) [50], all the Fc-containing PIL membranes are with excellent hemocompatibility.

The cell toxicity of the PIL membranes with adjustable antibacterial properties was characterized by MTT assay to evaluate the biocompatibility. The relative growth rates (RGRs) of the dermal fibroblast cells cultured with PIL membranes were evaluated by testing the OD values at 490 nm. As shown in Figure 5, the RGR values were 93.47%, 120.24%, 108.39%, and 109.42% for PIL-C_6-Fc, PIL-C_6-Fc^+, PIL-C_6-Fc-CD, PIL-C_6-Fc^+-CD membranes, respectively. The results indicated the redox-responsive PIL membranes were with none cell toxicity according to the

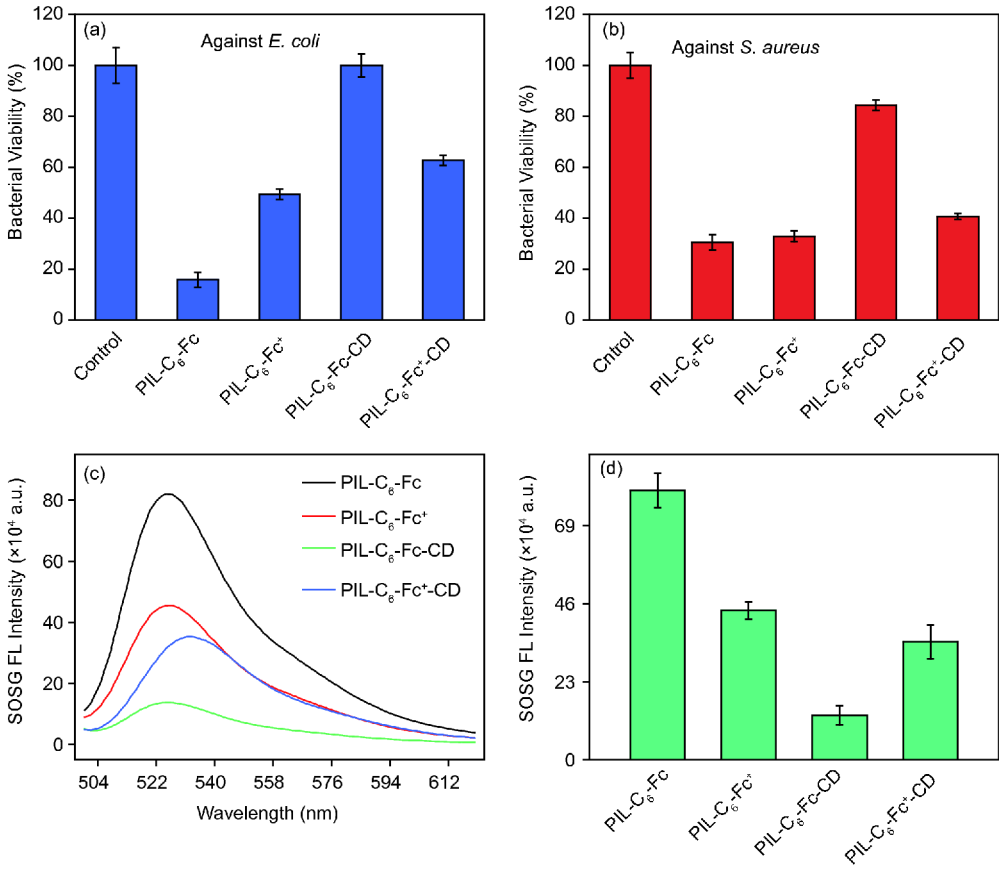

Figure 4 Antibacterial rate against (a) *E. coli* and (b) *S. aureus* after incubating with imidazolium-based PIL membranes under different modulated conditions for 4 h with PET membranes as the control. (c) The emission spectrums (λ_{ex}=494 nm) and (d) fluorescence intensity of SOSG (λ_{em}=530 nm) with the existence of PIL membranes in ultrapure water (color online).

Table 3 Hemolysis rate of the synthesized redox-responsive PIL membranes

Samples	Hemolysis rate (%)
PET	0.00±0.10
PIL-C_6-Fc	0.01±0.01
PIL-C_6-Fc^+	0.03±0.02
PIL-C_6-Fc-CD	0.03±0.02
PIL-C_6-Fc^+-CD	0.04±0.02

general acceptance criteria for biocompatibility of medical materials.

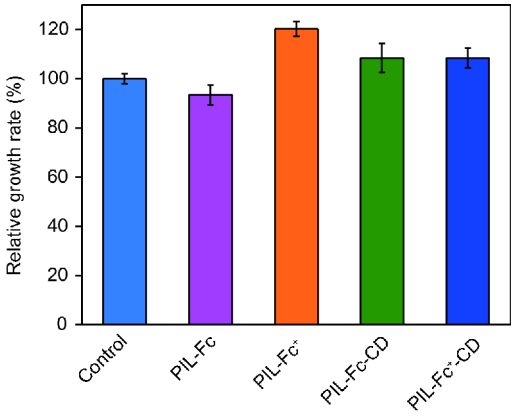

Figure 5 Cytotoxicity of the synthesized redox-reponsive PIL membranes (color online).

4 Conclusions

In conclusion, a series of redox-responsive Fc-containing imidazolium-based ILs and PIL membranes with tunable antibacterial activities were synthesized and applied for antibacterial applications. The antibacterial activities of the ILs were improved with the increased carbon chain length and the introduction of Fc groups. In addition, the antibacterial properties can be modulated by the redox state of the Fc as well as the host-guest interaction between Fc and β-CD. Both the oxidation of Fc to Fc^+, and the formation of inclusion complexes between Fc and β-CD led to the decline of the antibacterial activities. However, the antibacterial activities may be recovered in some extent if the Fc^+ was reduced to Fc or the exclusion of the Fc out of the cavity of β-CD. In addition, the redox-responsive tunable antibacterial activities

were also observed for imidazolium-based PIL membranes, which showed excellent blood compatibility and none cytotoxicity, demonstrating potential applications as eco-friendly antibacterial materials in the field of healthcare.

Acknowledgements This work was supported by the National Science Foundation for Distinguished Young Scholars (21425417), the National Natural Science Foundation of China (21704071), the Jiangsu Province Science Foundation for Youth (BK20170332), General Program Foundation of Jiangsu Province University Science Research Project (17KJB150033), General Program Foundation of Shanghai Municipal Commission of Health and Family Planning (201740107), and the Project Funded by the Priority Academic Program Development of Jiangsu Higher Education Institutions, and Science and Technology Innovation Fund Project of Zhongshan Hospital, Fudan University (2017ZSCX03).

Conflict of interest The authors declare that they have no conflict of interest.

Supporting information The supporting information is available online at http://chem.scichina.com and http://link.springer.com/journal/11426. The supporting materials are published as submitted, without typesetting or editing. The responsibility for scientific accuracy and content remains entirely with the authors.

1 Ng VWL, Ke X, Lee ALZ, Hedrick JL, Yang YY. *Adv Mater*, 2013, 25: 6730–6736
2 Tao WX, Zhu MH, Deng ZX, Sun YH. *Sci China Chem*, 2013, 56: 1364–1371
3 Miller AJM, Heinekey DM, Mayer JM, Goldberg KI. *Angew Chem Int Ed*, 2013, 52: 3981–3984
4 Sun Y, Sun G. *Macromolecules*, 2002, 35: 8909–8912
5 Jin JY, Ouyang XY, Li JS, Jiang JH, Wang H, Wang YX, Yang RH. *Sci China Chem*, 2011, 54: 1266–1272
6 Shah P, Yue Q, Zhu X, Xu F, Wang HS, Li CZ. *Sci China Chem*, 2015, 58: 1600–1604
7 Qin J, Guo J, Xu Q, Zheng Z, Mao H, Yan F. *ACS Appl Mater Interfaces*, 2017, 9: 10504–10511
8 Zheng Z, Xu Q, Guo J, Qin J, Mao H, Wang B, Yan F. *ACS Appl Mater Interfaces*, 2016, 8: 12684–12692
9 Cui H, Yuan L, Lin L. *Carbohydr Polymers*, 2017, 177: 156–164
10 Zhang J, He X, Zhang P, Ma Y, Ding Y, Wang Z, Zhang Z. *Sci China Chem*, 2015, 58: 761–767
11 Long Y, Wang Y, Liu Y, Zeng Q, Li Y. *Sci China Chem*, 2015, 58: 666–672
12 Wang L, Su B, Cheng C, Ma L, Li S, Nie S, Zhao C. *J Mater Chem B*, 2014, 3: 1391–1404
13 Yang Z, Yu H, Zhang L, Wei H, Xiao Y, Chen L, Guo H. *Chem Asian J*, 2014, 9: 313–318
14 Sundararaman M, Rajesh Kumar R, Venkatesan P, Ilangovan A. *J Med Microbiol*, 2013, 62: 241–248
15 Huang Y, Pappas HC, Zhang L, Wang S, Cai R, Tan W, Wang S, Whitten DG, Schanze KS. *Chem Mater*, 2017, 29: 6389–6395
16 Chait R, Craney A, Kishony R. *Nature*, 2007, 446: 668–671
17 Zhang Q, Lambert G, Liao D, Kim H, Robin K, Tung C, Pourmand N, Austin RH. *Science*, 2011, 333: 1764–1767
18 Huang Z, Zhang H, Bai H, Bai Y, Wang S, Zhang X. *ACS Macro Lett*, 2016, 5: 1109–1113
19 Bai H, Zhang H, Hu R, Chen H, Lv F, Liu L, Wang S. *Langmuir*, 2017, 33: 1116–1120
20 Bai H, Fu X, Huang Z, Lv F, Liu L, Zhang X, Wang S. *Chemistryselect*, 2017, 2: 7940–7945
21 Bai H, Yuan H, Nie C, Wang B, Lv F, Liu L, Wang S. *Angew Chem Int Ed*, 2015, 54: 13208–13213
22 Wei T, Zhan W, Cao L, Hu C, Qu Y, Yu Q, Chen H. *ACS Appl Mater Interfaces*, 2016, 8: 30048–30057
23 Subianto S, Mistry MK, Choudhury NR, Dutta NK, Knott R. *ACS Appl Mater Interfaces*, 2009, 1: 1173–1182
24 Mehta MJ, Kumar A. *Chem Asian J*, 2017, 12: 3150–3155
25 Chin W, Yang C, Ng VWL, Huang Y, Cheng J, Tong YW, Coady DJ, Fan W, Hedrick JL, Yang YY. *Macromolecules*, 2013, 46: 8797–8807
26 Szente L, Puskás I, Csabai K, Fenyvesi É. *Chem Asian J*, 2014, 9: 1365–1372
27 Sun Z, Liu X, Guo J, Xu D, Shen S, Yan F. *Chem Asian J*, 2017, 12: 2950–2955
28 Wang XC, Wu JY, Zhou HP, Tian YP, Li L, Yang JX, Jin BK, Zhang SY. *Sci China Ser B-Chem*, 2009, 52: 930–936
29 Li SH, Wu CY, Lv XY, Tang X, Zhao XQ, Yan H, Jiang H, Wang XM. *Sci China Chem*, 2012, 55: 2388–2395
30 Li SH, Wu CY, Tang X, Gao SP, Zhao XQ, Yan H, Wang XM. *Sci China Chem*, 2013, 56: 595–603
31 Xu G, Pranantyo D, Xu L, Neoh KG, Kang ET, Teo SLM. *Ind Eng Chem Res*, 2016, 55: 10906–10915
32 Lewandowski EM, Szczupak Ł, Wong S, Skiba J, Guśpiel A, Solecka J, Vrček V, Kowalski K, Chen Y. *Organometallics*, 2017, 36: 1673–1676
33 Savjani KT, Gajjar AK, Savjani JK. *ISRN Pharm*, 2012, 2012: 1–10
34 Chaudhary VB, Patel JK. *Int J Pharm Sci Res*, 2013, 4: 68–76
35 Kumar S, Bhargava D, Thakkar A, Arora S. *Crit Rev Ther Drug Carrier Syst*, 2013, 30: 217–256
36 Svenson S, Chauhan AS. *Nanomedicine*, 2008, 3: 679–702
37 Yuan C, Guo J, Tan M, Guo M, Qiu L, Yan F. *ACS Macro Lett*, 2014, 3: 271–275
38 Cao D, Liu W, Wei X, Xu F, Cui L, Cao Y. *Tissue Eng*, 2006, 12: 1369–1377
39 Locock KES, Michl TD, Stevens N, Hayball JD, Vasilev K, Postma A, Griesser HJ, Meagher L, Haeussler M. *ACS Macro Lett*, 2014, 3: 319–323
40 Pu F, Liu X, Xu B, Ren J, Qu X. *Chem Eur J*, 2012, 18: 4322–4328
41 Li P, Zhou C, Rayatpisheh S, Ye K, Poon YF, Hammond PT, Duan H, Chan-Park MB. *Adv Mater*, 2012, 24: 4130–4137
42 Gabriel GJ, Som A, Madkour AE, Eren T, Tew GN. *Mater Sci Eng-R-Rep*, 2007, 57: 28–64
43 Fischer W. *Med Microbiol Immunol*, 1994, 183: 61–76
44 Patra M, Gasser G, Wenzel M, Merz K, Bandow JE, Metzler-Nolte N. *Organometallics*, 2010, 29: 4312–4319
45 Beveridge TJ. *J Bacteriol*, 1999, 181: 4725–4733
46 Palermo EF, Sovadinova I, Kuroda K. *Biomacromolecules*, 2009, 10: 3098–3107
47 Acevedo-Morantes CY, Melendez E, Singh SP, Ramirez-Vick JE. *J Cancer Sci Ther*, 2012, 4: 271–275
48 Nakahata M, Takashima Y, Yamaguchi H, Harada A. *Nat Commun*, 2011, 2: 511
49 Lin B, Qiu L, Lu J, Yan F. *Chem Mater*, 2010, 22: 6718–6725
50 Nederberg F, Zhang Y, Tan JPK, Xu K, Wang H, Yang C, Gao S, Guo XD, Fukushima K, Li L, Hedrick JL, Yang YY. *Nat Chem*, 2011, 3: 409–414